JACS
JOURNAL OF THE AMERICAN CHEMICAL SOCIETY

Article

Chemical Synthesis Enables Structural Reengineering of Aglaroxin C Leading to Inhibition Bias for HCV Infection

Wenhan Zhang, Shufeng Liu, Rayelle I Maiga, Jerry Pelletier, Lauren E. Brown, Tony T. Wang, and John A. Porco

J. Am. Chem. Soc., **Just Accepted Manuscript** • DOI: 10.1021/jacs.8b11477 • Publication Date (Web): 27 Dec 2018

ACS Publications

is published by the American Chemical Society. 1155 Sixteenth Street N.W., Washington, DC 20036

Chemical Synthesis Enables Structural Reengineering of Aglaroxin C Leading to Inhibition Bias for HCV Infection

Wenhan Zhang,[a‡] Shufeng Liu,[b‡] Rayelle I. Maiga,[c] Jerry Pelletier,[c, d, e] Lauren E. Brown,[a] Tony T. Wang,[b]* and John A. Porco, Jr.[a]*

[a] Department of Chemistry, Center for Molecular Discovery (BU-CMD), Boston University, Boston, MA 02215, USA

[b] Laboratory of Vector-borne Viral Diseases, Division of Viral Products, Center for Biologics Evaluation and Research, Food and Drug Administration, Silver Spring, MD 20903, USA

[c] Department of Biochemistry, [d] Department of Oncology, [e] Rosalind & Morris Goodman Cancer Research Centre, McGill University, Montreal, Quebec, H3G1Y6, Canada

KEYWORDS aglaroxin, natural product synthesis, late-stage modification, viral entry, HCV, rocaglate, natural product analogues, inhibition bias.

ABSTRACT: As a unique rocaglate (flavagline) natural product, aglaroxin C displays intriguing biological activity by inhibiting HCV viral entry. To further elucidate structure-activity relationships and diversify the pyrimidinone scaffold, we report a concise synthesis of aglaroxin C utilizing a highly regioselective pyrimidinone condensation. We have prepared more than forty aglaroxin C analogues utilizing various amidine condensation partners. Through biological evaluation of analogues, we have discovered two lead compounds, CMLD012043 and CMLD012044, which show preferential bias for the inhibition of HCV viral entry *vs*. translation inhibition. Overall, the study demonstrates the power of chemical synthesis to produce natural product variants with both target inhibition bias and improved therapeutic indexes.

INTRODUCTION

Rocaglates (flavagline) natural products were first isolated from the dried roots and stems of *Aglaia elliptifolia* Merr. (family Meliaceae) in 1982.[1] Since then, over thirty rocaglate natural products have been identified with unique structures and intriguing biological activities.[2, 3, 4] For instance, silvestrol (**1**, Figure 1)[5] was identified as an excellent translation inhibitor for cancer chemotherapy,[6] whereas other related natural products and analogues (**2**-**4**) displayed similar activities.[7] In our previous studies, translation inhibition was found to be associated with inhibition of the DEAD box RNA helicase eIF4A.[8] Owing to the interesting structures and biological activities of rocaglates, a number of total syntheses[9] and medicinal chemistry studies[10, 11] have been disclosed. Our group has a long-standing interest in the synthesis of rocaglates and derivatives as well as investigations of their biology.[6, 7, 8, 9g, i, k, o-q, 10a, c, e-f] In 2015, we reported the enantioselective synthesis of aglaiastatin (**5**) and aglaroxin C (**6**) through biomimetic kinetic resolution.[9p] Subsequent studies revealed that **5** was a promising translation inhibitor. In contrast, **6**, containing a fully substituted pyrimidinone core, showed only moderate translation inhibition.[9p] In separate studies, we discovered that **6** inhibited hepatitis C viral (HCV) entry into host cells at a low μM concentration, potentially through inhibition of the prohibitins (PHBs) as viral entry factors.[12, 13] Notably, prohibitins 1 and 2 have been reported as general viral entry factors for other viruses including dengue virus type 2 (DENV-2)[14] and Chikungunya.[15] We were further encouraged by the observation that **6** did not induce cytotoxicity by translation inhibition at a concentration that is effective for inhibition of viral entry, providing a promising therapeutic index (TI) for potential treatment of HCV infection.[12]

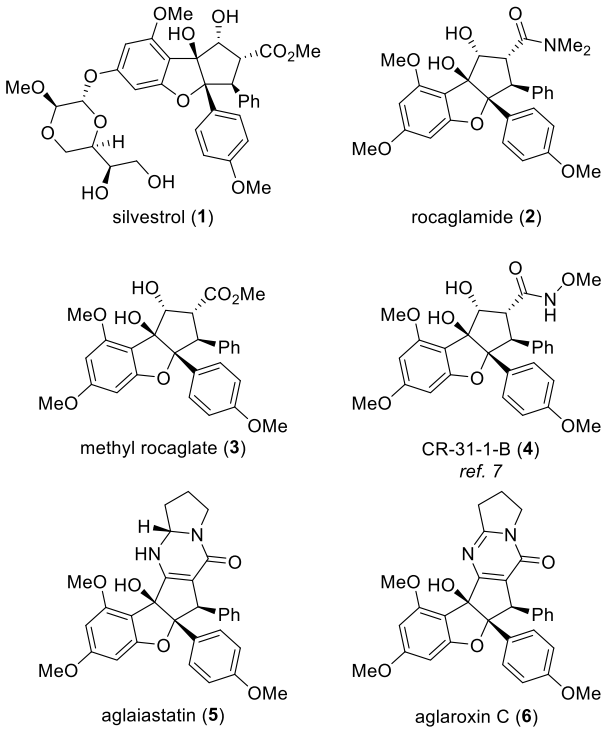

Figure 1. Representative Biologically Active Rocaglate Natural Products and Synthetic Analogues

Scheme 1. First-Generation Synthesis of Aglaroxin C Using Stepwise Pyrimidinone Formation

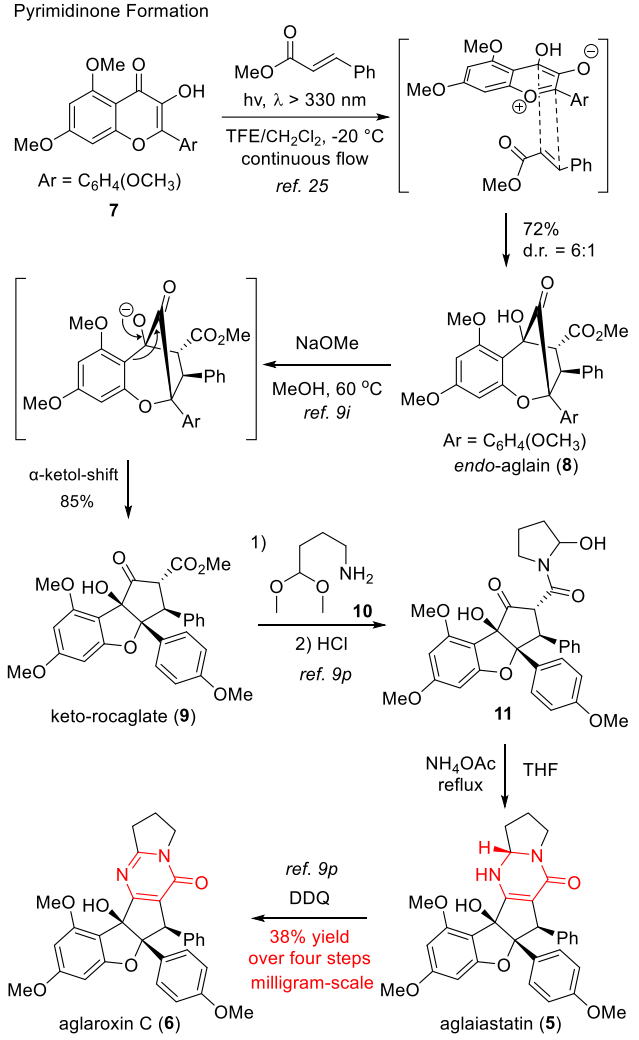

HCV is a widespread viral pathogen. The recent estimated number of viral carriers is 143 million worldwide,[16] and over 2% of the population in North America has been infected. In addition, chronic HCV infection causes severe liver diseases in carriers, including liver cancer and cirrhosis.[17] In 2015, over a half million people died from diseases due to HCV infection.[18] Recently, direct-acting antiviral agents (DAAs) have become available to cure HCV infection[19] by inhibiting the function of non-structural (NS) viral proteins. However, treatment effects of DAAs vary across different genotypes of HCV, and HCV potentially may develop resistance to these agents.[20] For example, the NS3 protease inhibitor simeprevir only treats genotypes 1 and 4 of HCV, and several signature resistance mutations have been identified against this treatment.[21] Sofosbuvir, a top NS5B inhibitor, failed in HCV treatment which was associated with resistance mutations (Figure SI1).[22] Accordingly, discovery of alternative treatments for HCV is sorely needed. As PHB-mediated cellular signaling pathways[12] are required by all HCV genotypes to infect host cells, it is conceivable that a small molecule such as aglaroxin C (**6**) may block infection from multiple HCV genotypes.[23] Additionally, targeting the host component for viral entry may create higher genetic barriers against resistance.[24] Lastly, aglaroxin C and analogues may also be valuable for dissecting the mechanisms of HCV entry and may inhibit other viruses sharing the same entry mechanism.

Scheme 2. Retrosynthetic Analysis for Aglaroxin C Analogues

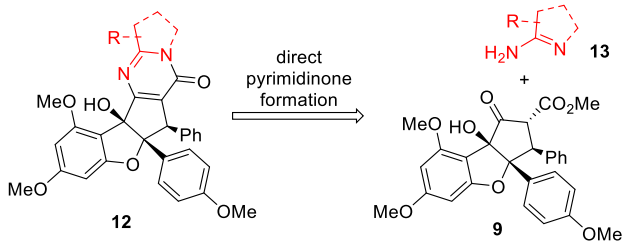

Our goal was to reengineer the structure of aglaroxin C (**6**) to

Table 1. Optimization of the Direct Pyrimidinone Formation

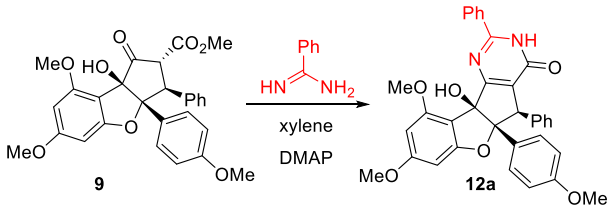

Entry	DMAP (equiv)	amidine (equiv)	Conc. (M)	Temp. (°C)	time (hour)	NMR yield (%) **12a** ; **14** ; **15** ; **16**
1	0.2	10.0	0.2	130[a]	1	28 , - , 9 , -
2	1.5	3.0	0.2	120	12	27 , - , 8 , 51
3	0.3	3.0	0.2	120	12	68 , 4 , 13 , 11
4	0.3	1.0	0.2	120	12	62 , 13 , 2 , 11[b]
5	0.3	-	0.2	120	12	- , 54 , - , -[c]
6	0.3	2.0	0.025	120	12	81 , 5 , 5 , 8
7	0.3	1.8	0.025	130	24	55 , 11 , - , 30
8	0.3	3.0	0.025	130	0.75	**90** , - , - , **5**[d]
9	-	3.0	0.025	130	0.75	**86** , - , - , **6**[e]

Side Products:

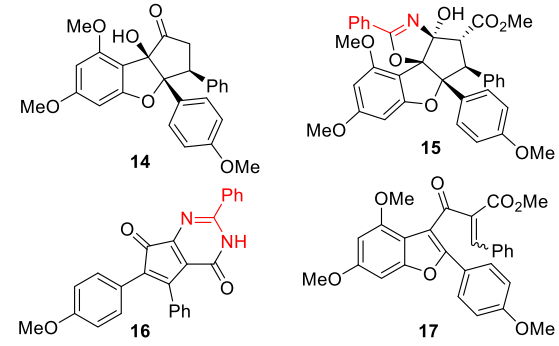

[a]*Microwave,* toluene as solvent; [b]10% of **9** recovered; [c]20% of **9** recovered, 24% yield of **17**; [d]81% isolated yield of **12a**; [e]78% isolated yield of **12a**.

increase activity against HCV entry while minimizing translation inhibition, which may lead to undesired cytotoxicity.[5, 6, 7, 8] As the oxidation state change between **6** and aglaiastatin (**5**) led to different biological profiles, we speculated that the pyrimidinone subunit of **6** may be important for inhibition of HCV viral entry *vs.* translation inhibition. Our first-generation synthesis of aglaroxin C (**6**) utilized a key intermediate, keto-rocaglate **9**,[25] which was synthesized through the excited state intramolecular proton transfer (ESIPT) [3+2] cycloaddition between 3-hydroxyflavone **7** and methyl cinnamate followed by α-ketol shift of the aglain intermediate **8** (Scheme 1).[9i] However, the late stage pyrimidinone synthesis in our first-generation synthetic

route is not ideal for rapid analog synthesis, affording **6** in low yield on a multi-milligram scale (Scheme 1).[26] We also envisioned that stepwise pyrimidinone synthesis may suffer from poor functional group tolerance in analogues due to the use of both acidic and oxidative conditions. Moreover, use of tethered aminoacetals such as **10** in the ester-amide exchange to produce intermediate **11** considerably narrows the diversity of accessible analogues due to limited availability of such building blocks. We therefore considered a streamlined synthesis of aglaroxin analogues through late stage, one-step pyrimidinone formation (Scheme 2).

RESULTS AND DISCUSSION

Development of a Direct Pyrimidinone Formation. Our second-generation synthetic route (Scheme 2), which relies on condensation of keto-rocaglate (**9**) with commercially available amidines **13**, was expected to flexibly provide analogues (**12**) for biological experiments. Pyrimidinones have served as biologically important substructures in both drugs and natural products.[27, 28] There are many well-established and practical methods for the synthesis of pyrimidinones and pyrimidines, including the Traube synthesis of purines,[29] which inspired us to consider late stage construction of the pyrimidinone core of aglaroxin analogues.[30] However, we anticipated that condensation between the structurally complex substrate **9** and amidines **13** would be challenging. In particular, the highly ionizable tertiary, benzylic alcohol adjacent to the ketoester moiety may provide unexpected reactivity under the reaction conditions.

Our initial model study for pyrimidinone formation employed benzamidine as a simplified condensation partner. Microwave conditions (Table 1, entry 1) produced minimal amounts of pyrimidinone **12a** in an unsatisfactory yield of 28% (determined by ^{1}H NMR analysis) due to low conversion.[9p] Thermal conditions (entry 2) resulted in full consumption of **9**, while cyclopentapyrimidinedione **16** and 3,5-dimethoxyphloroglucinol were found as the major identified side products. The formation of fragmentation product **16** was found to correlate with the amount of 4-dimethylaminopyridine (DMAP) employed; reduction to 0.3 equivalents of DMAP minimized

Scheme 3. Possible Mechanistic Pathways and Products of Direct Pyrimidinone Formation.

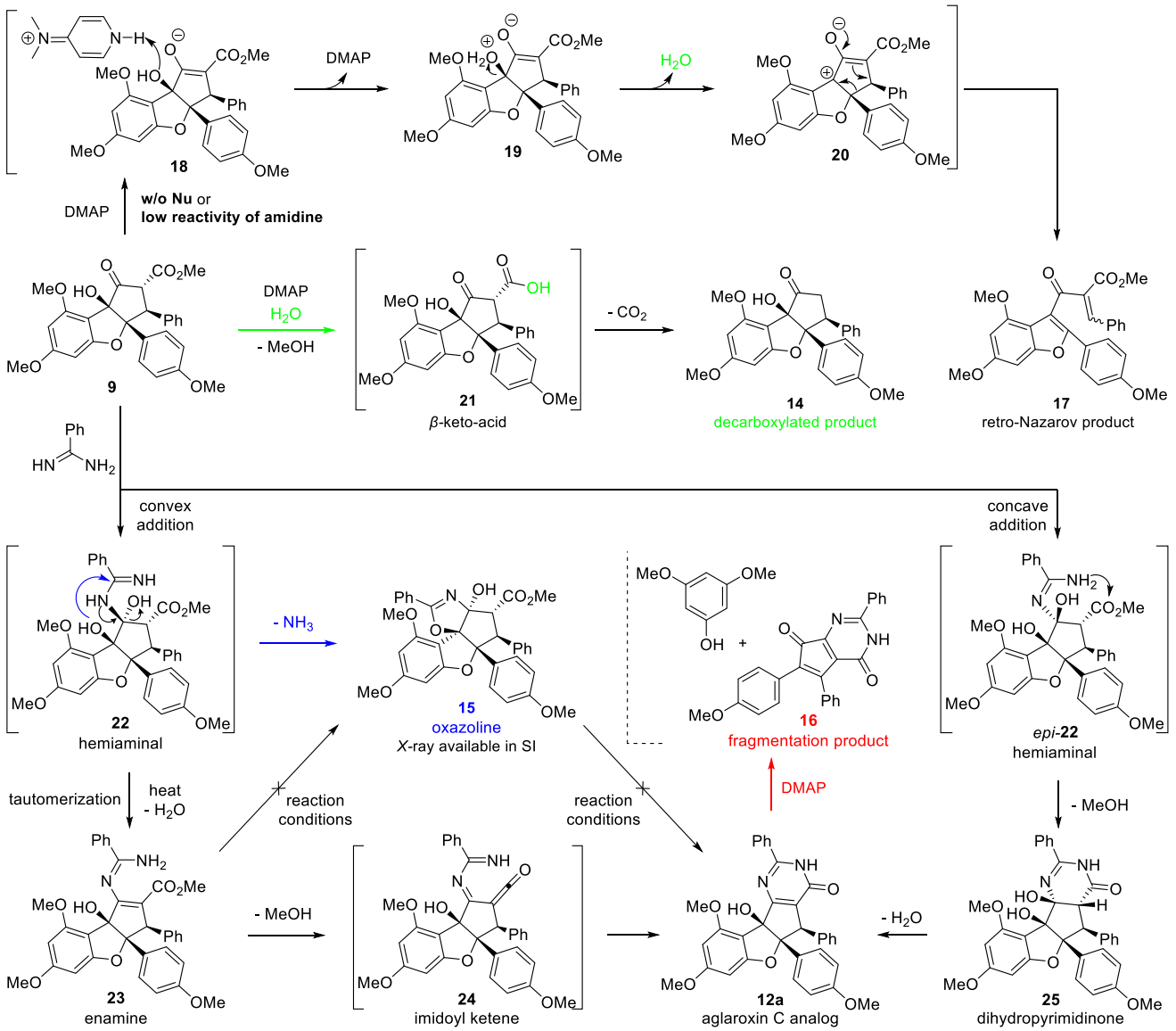

production of **16** (entry 3) but also led to formation of an unexpected cyclization product, oxazoline **15**. The structure of **15** was confirmed by single crystal X-ray crystal structure analysis.[26] Reduced equivalents of the benzamidine reaction partner resulted in an incomplete reaction, with increased production of decarboxylation product **14** and retro-Nazarov products **17** (entries 4 & 5).[26] We next found that diluting the reaction eightfold improved the yield of **12a** (entry 6). Increasing both temperature and reaction time under dilute conditions eliminated the production of **15**, but also led to a lower yield of **12a** in favor of significant amounts of **16** (entry 7). Gratifyingly, by reducing the reaction time to 45 minutes, we obtained a 90% NMR yield of **12a** with minimal fragmentation to **16** (entry 8); ultimately, an 81% isolated yield of **12a** was obtained on a 100-mg scale. Interestingly, we found that the model reaction gave the almost identical yield in absence of DMAP under the optimized conditions (entry 9), but we acheived better reproducibility when amidine hydrochloride salt was used with DMAP (*vide infra*).

Proposed Mechanistic Pathway. According to trends observed during reaction optimization, we propose the mechanistic pathway depicted in Scheme 3. We postulate that water generated from the pyrimidinone condensation may hydrolyze **9** to the *β*-keto-acid intermediate **21**, which undergoes decarboxylation to ketone **14**. When no nucleophile was used, **14** and retro-Nazarov product **17** were obtained. Presumably DMAP may promote intramolecular proton transfer to **19** followed by the extrusion of water to afford the retro-Nazarov precursor **20**, whereas the formed water triggered decarboxylation of **9** (an alternative mechanism is shown in the SI). In the presence of the amidine, the desired formation of hemiaminals **22** and *epi*-**22** appears to compete with decarboxylation and retro-Nazarov reaction, which can be enhanced through use of increased equivalents of the amidine. Based on the Katrizky mechanism determined for the Traube reaction of *β*-keto esters and amidines,[31] two possible pathways may be envisioned for the formation of pyrimidinone **12a**. In one mechanism, hemiaminal *epi*-**22**, generated from disfavored concave-addition of the amidine to **9**,[9i] may cyclize to dihydropyrimidinone **25** followed by extrusion of water. In contrast, hemiaminal **22**, obtained from amidine addition to the convex face of **9**, has an *anti*-relationship between the aminal and ester thereby preventing direct cyclization. Instead, loss of water would produce the observed enamine **23**, which we propose then cyclizes to **12a** through extrusion of methanol generating imidoyl ketene **24** followed by a 6π-electrocyclization to pyrimidinone **12a**.[32] To support the formation of hemiaminal **22**, the oxazoline byproduct **15** was formed through cyclization of the tertiary alcohol of **22** to the amidine carbon followed by extrusion of ammonia (blue arrow). The formation of **22** is also supported by our isolation of enamine **23** from a 250 mg scale reaction, where a 28% yield of **23** was found to precipitate after 10 minutes; we subsequently found that **23** can also be synthesized in 60% yield using **9** and benzamidine at 60 ℃ in toluene.[26] Interestingly, isolated **23** was found to solely produce **12a** with no observed formation of **15** when **23** was resubjected to the reaction conditions. We rationalize that the sp^3-hybridized hemiaminal carbon of **22** allows for a conformation necessary for intramolecular cyclization, whereas the sp^2-hybridized enamine carbon of **23** prevents a similar cyclization. This conforms to the observation that elevated temperatures facilitate extrusion of water generating

Table 2. Optimization of Second-Generation Synthesis of Aglaroxin C

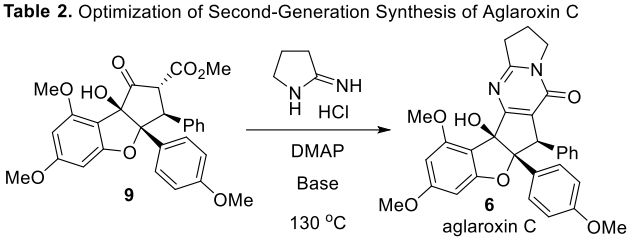

Entry	base (equiv)	amidine (equiv)	DMAP (equiv)	solvent	NMR yield (%)
1	DBU (4.0)	2.1	-	EtOH[a]	-[b]
2	MeONa (11.6)	10.0	0.1	toluene[a]	-[b]
3	MeONa (0.75)	1.5	0.1	toluene[a]	-[b]
4	MeONa (9.8)	10.0	1.5	toluene[a]	19
5	MeONa (4.9)	5.0	1.5	toluene[c]	-[d]
6	MeONa (2.95)	3.0	0.4	xylene[e]	86[f]

[a]0.025 M concentration, reflux 12 h; [b]no conversion; [c]0.2 M concentration, reflux 12 h; [d]complex reaction; only isolated the fragmentation products; [e]0.025 M concentration, 130 °C 1 h; [f]76% isolated yield for aglaroxin C; 9% decarboxylated product also obtained.

enamine **23** and minimize formation of byproduct **15**. In contrast, **15** did not generate **12a** under the reaction conditions. In a control experiment, DMAP was found to accelerate the fragmentation of **12a** into **16** and 3,5-dimethoxyphloroglucinol.[26]

Second-Generation Synthesis of Aglaroxin C. After determining optimal conditions for direct pyrimidinone formation, we next sought to apply these conditions to synthesize aglaroxin C (**6**). In this case, the requisite pyrrolidin-2-imine was commercially available as an HCl salt (Table 2). Initial attempts using stepwise free-basing protocols failed due to the high-water solubility of the amidine; accordingly, we focused on *in-situ* free-basing conditions for optimization studies. Using excess base (entries 1 and 2), no conversion of substrate **9** was observed after refluxing for 12 h. As **9** exists as mixture of enol/keto isomers, presumably excess base favors formation of an unreactive enolate. In contrast, use of excess pyrrolidin-2-imine HCl salt (entry 3) did not induce pyrimidinone formation. We assume that DMAP is protonated by the amidine salt which negated its function. When a slight excess of amidine *vs*. NaOMe (entry 4) was used, we obtained **6** in 19% isolated yield. Consistent with our earlier optimization efforts, use of increased concentration and 12 h reaction time resulted in a complex reaction mixture containing fragmentation products (entry 5). Finally, use of 3.0 equiv. of amidine salt and 2.95 equiv. of NaOMe along with a catalytic amount of DMAP (40 mol%, 130 °C) afforded **6** in 76% isolated yield on a 100-mg scale (entry 6).

Synthesis of Aglaroxin Analogues. With reliable annulation protocols available using both amidines and amidine salts, we next synthesized a library of aglaroxin analogues (Table 3). In general, direct pyrimidinone formation was found to tolerate both aromatic and aliphatic amidines. We observed consistent yields for formation of *C*-substituted pyrimidinones (**12b**-**12f**). For instance, simple aliphatic amidines reacted with **9** to afford

Table 3. Synthese of Aglaroxin C Analogues Using Direct Pyrimidinone Formation[a]

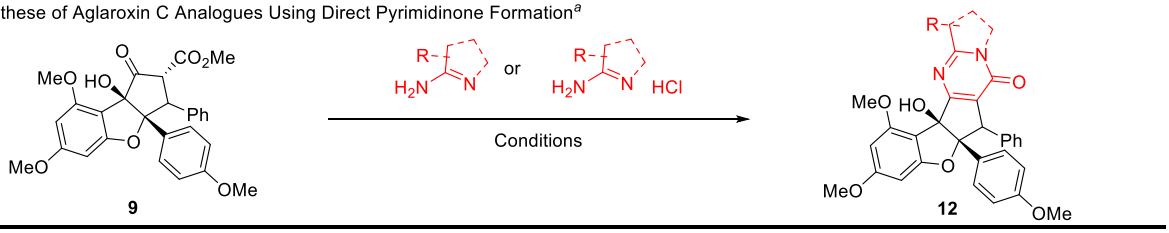

	R^1	yield
12a	Ph	80%[b]
12b	Me	69%
12c	Bn	47%
12d	^{i}Pr	87%
12e	Cy	96%
12f	H	53%

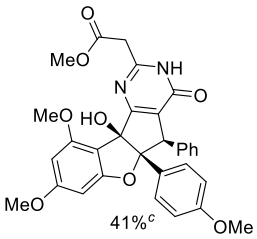

12g

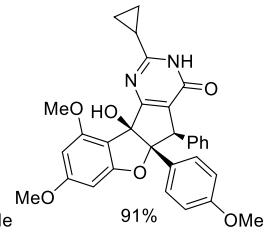

12h

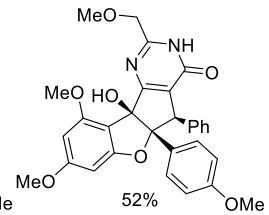

12i

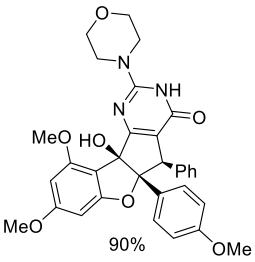

12j

	R^2	yield
12k	OMe	83%
12l	Me	66%[b]
12m	OBn	68%
12n	NMe_2	82%
12o	CF_3	53%

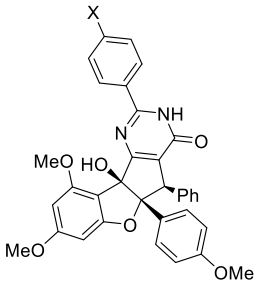

	X	yield
12p	F	79%
12q	Cl	78%
12r	Br	75%

	R^3	yield
12s	OMe	73%[b]
12t	Me	74%
12u	OBn	71%

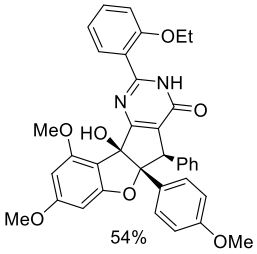

12v

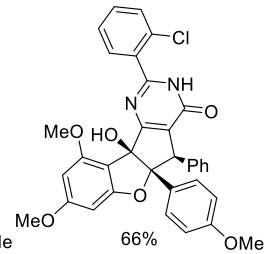

12w

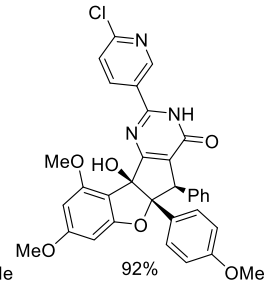

12x

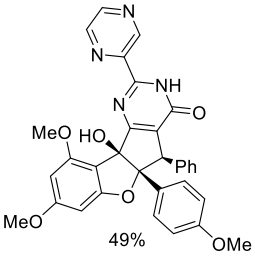

12y

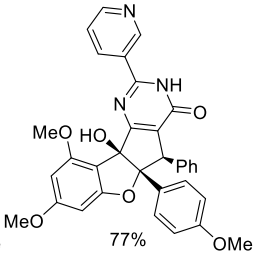

12z

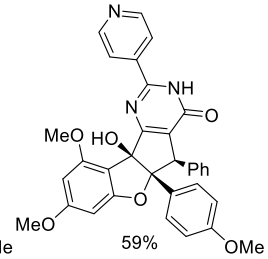

12aa

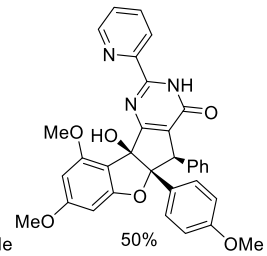

12ab

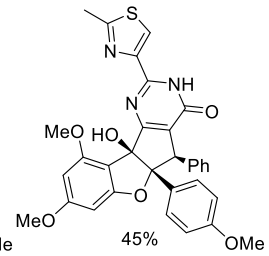

12ac

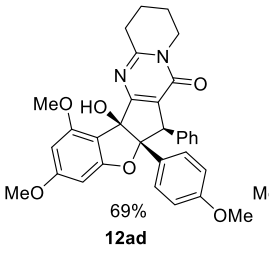

12ad

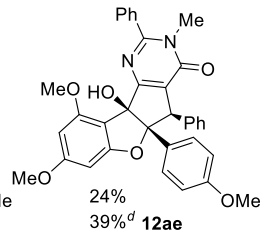

12ae

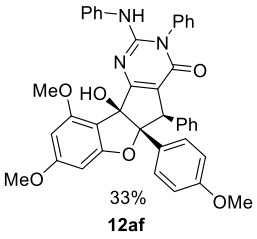

12af

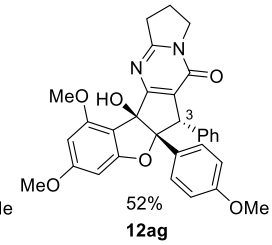

12ag

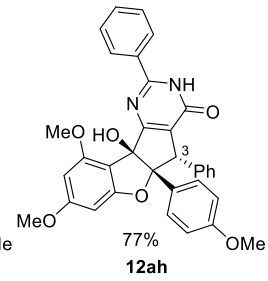

12ah

[a]Standard conditions: 25 mg of **9**, 3 equiv amidine, 0.3 equiv DMAP, *m*-xlyene (0.025 M), 130 °C, 45 min; 2.95 equiv NaOMe (1.0 M in MeOH) was used for amidine salts; [b]250 mg of **9** was used; [c]ethyl 2-amidinoacetate HCl salt was used, and 8% of the ethyl ester product was isolated; [d]*m*-xlyene (0.2 M).

C-Me (**12b**) and *C*-Bn (**12c**) pyrimidinones. Hindered amidines

such as *iso*-butanamidine and cyclohexylcarboxamidine afforded the desired products **12d** and **12e** in excellent yields. Interestingly, condensation of carbomethoxyformamidine with **9** was followed by an unexpected decarboxylation to produce the non-substituted product **12f** in 53% yield. Moreover, we discovered that the pyrimidinone condensation could tolerate various functional groups, including ester **12g** (41%), cyclopropane **12h** (91%), and methoxyl methylene **12i** (52%). Ester exchange was observed when ethyl amidinoacetate was employed, producing compound **12g**. Additionally, guanidine-type reaction partners successfully underwent condensation, yielding products such as **12j** (90% yield).

Preliminary biological studies of the analog set indicated that *C*-aryl pyrimidinones consistently possessed good inhibition of HCV infection with low cytotoxicity (*vide infra*).[26] Accordingly, we synthesized additional *C*-aryl pyrimidinone analogues with a variety of substitution patterns, with an initial focus on *para*-substituted aryl benzamidines (Table 3, **12k-r**). Generally, condensations tolerated both electron-rich and deficient benzamidines; however, we found that greater amounts of fragmentation products were generated using electron-deficient amidines (*cf.* compounds **12k-n** 66-83% yield) with compound **12o**, which was generated in 53% yield along with the corresponding fragmentation products. Compound **12m** was further subjected to hydrogenolysis to afford the free phenol which may serve as a potential handle for further modifications.[26] As expected, analogues including *para*-halides (**12p**-**12r**) were synthesized in 70-80% yields. Such compounds may also allow for late stage functionalization *via* aminations and S_NAr reactions. We found that *meta*-substituted benzamidines were also workable, affording products (**12s**-**12u**) using the standard protocol in reasonable yields (71%-73%). Using the sterically hindered *ortho*-substituted benzamidines, **12v** and **12w** were synthesized in moderate yields (54% and 66%). Six *C*-heteroaryl substituted analogues (**12x**-**12ac**) were also synthesized; in these cases, we observed substantial fragmentation of the desired products. Only **12x** and **12z** were obtained in reasonable yields (92% and 77%, respectively), while compounds **12y** and **12aa**-**12ac** were obtained in yields averaging 50%.

As we found that aglaroxin C (**6**, Table 2) was synthesized regioselectively using an unsymmetrical amidine, we also tested additional unsymmetrical amidines in the pyrimidinone formation. Among all products formed, we found that the *N*-substituent was situated exclusively on the nitrogen adjacent to the pyrimidinone carbonyl (**12ad**-**af**). During the synthesis of **12ae**, a small amount of oxazoline **15** was obtained as the only observable side product. This result supports our mechanistic proposal (*cf.* Scheme 3) wherein the less sterically hindered, unsubstituted nitrogen likely engages in initial hemiaminal formation with **9**. Along these lines, we also synthesized **12ac**, a ring-expanded analog of **6**, in 69% yield. Unlike **12ad,** adducts **12ae** and **12af** were synthesized in 24 and 33% yields, respectively; these reactions generated significant amounts of retro-Nazarov and decarboxylated products, suggestive of lower overall reactivities among the *N*-substituted amidines.[26] We also optimized the yield of **12ae** to 39% by increasing the reaction concentration to 0.2 M. Finally, using *exo*-keto-rocaglate as the starting material, we synthesized compounds **12ah** and **12ag**, the C-3 epimers of **12a** and **6**, in 77 and 52% yields, respectively.

As a comparison to the direct condensation with unsymmetrical amidines, we also attempted alkylations of **12a** to produce compounds **12ai-aj** (Table 4) **12al**-**an** (see Supporting Information).[26] Unfortunately, all attempted alkylations displayed poor chemo- and regioselectivity, favoring the undesired *O*-alkylation products such as *O*-methoxypyrimidine **12ai**.

BIOLOGICAL STUDIES

Structure-Activity Relationships. We next evaluated the library of (±)-aglaroxin analogues and side products against HCV infection, and also tested their corresponding cytotoxicity in human hepatic (Huh) 7.5.1 cells.[26] In comparison to aglaroxin C (**6**), *C*-alkyl substituted pyrimidinones **12b-d** and **12h** (Table 3) exhibited increased inhibition against HCV infection, whereas **12e-g** had decreased activities. Nevertheless, the *C*-aryl substituted products (**12a**, **k-w**) showed a promising increase of inhibition of HCV infection with similar or reduced cytotoxicity in comparison to **6**. Excitingly, **12l** (CMLD012043) and **12s** (CMLD012044) showed a three-fold greater inhibition of HCV infection in comparison to **6**, while **12l** and **12s** exhibited relatively low cytotoxicity to Huh-7.5.1 cells (less than 50% cell death at 200 μM). Thus, the two lead compounds (**12l** and **12s**) provided excellent selectivity indexes (SI) in inhibiting HCV infection (*vide infra*). Notably, among all the *C*-heteroaryl substituted aglaroxin analogues (**12x**-**12ac**), only **12y** and **12ab** displayed slightly increased inhibition of HCV infection relative to **6**. The six-membered ring analog **12ad** and guanidine-type adducts **12j** and **12af** were found to have moderate antiviral activity.

To further understand structure-activity relationships (SAR) among aglaroxin analogues, we highlight ten compounds in Table 4 along with dose-response curves depicting their effectiveness in both HCV infection and cytotoxicity assays. As a benchmark compound, **6** was found to inhibit HCV infection with an EC_{50} of 1.3 μM and showed a CC_{50} of 12 μM. Of note, EC_{50} and CC_{50} values were calculated according to the fitted sigmoid curves, which are reported as absolute values (indicating the concentration of compounds providing 50% inhibition and 50% cell death, respectively). Next, we compared the EC_{50} of cyclohexyl- (**12e**) and phenyl-substituted (**12a**) pyrimidinones and found that *C*-aryl substitutions led to improved potency against viral infection (420 nM *vs*. 2.5 μM). The C-3 epimer (**12ah**) of **12a** was found to be inactive against HCV infection and no cytotoxicity. It is apparent that a *syn*-relationship of the two aryl rings on the cyclopenta[*b*]benzofuran core is crucial for HCV inhibition.

Based on the observation that *N*-methylated isomer **12ae** was one-fold more active than **12a** (EC_{50} 0.2 μM *vs.* 0.42 μM) with similar cytotoxicities (CC_{50} 7.3 μM *vs*. 8.1 μM),[33] we next utilized methylation to evaluate other sites for introduction of target identification tags. In contrast to *N*-methylation, we observed a decrease in inhibition of HCV infection (EC_{50} = 9.2 μM) with the *O*-methylated pyrimidine **12ai**. The doubly methylated product **12aj** was also found inactive and non-toxic. Finally, we studied the impact of substituting the conjugated *C*-aryl group of the pyrimidinone (*cf.* **12l**, **12o**, and **12s**). Compound **12o,** with an electron-withdrawing CF_3-group, had higher cytotoxicity (CC_{50} = 10 μM), and only a one-fold better EC_{50} (0.24 μM) for HCV inhibition than **12l** and **12s** (EC_{50} ~ 0.5 μM). The two lead compounds **12l** and **12s** displayed im-

Table 4. Structure-Activity Relationship of Racemic Aglaroxin C Analogues in the HCV Infection Inhibition and cytotoxicity Assays[a]

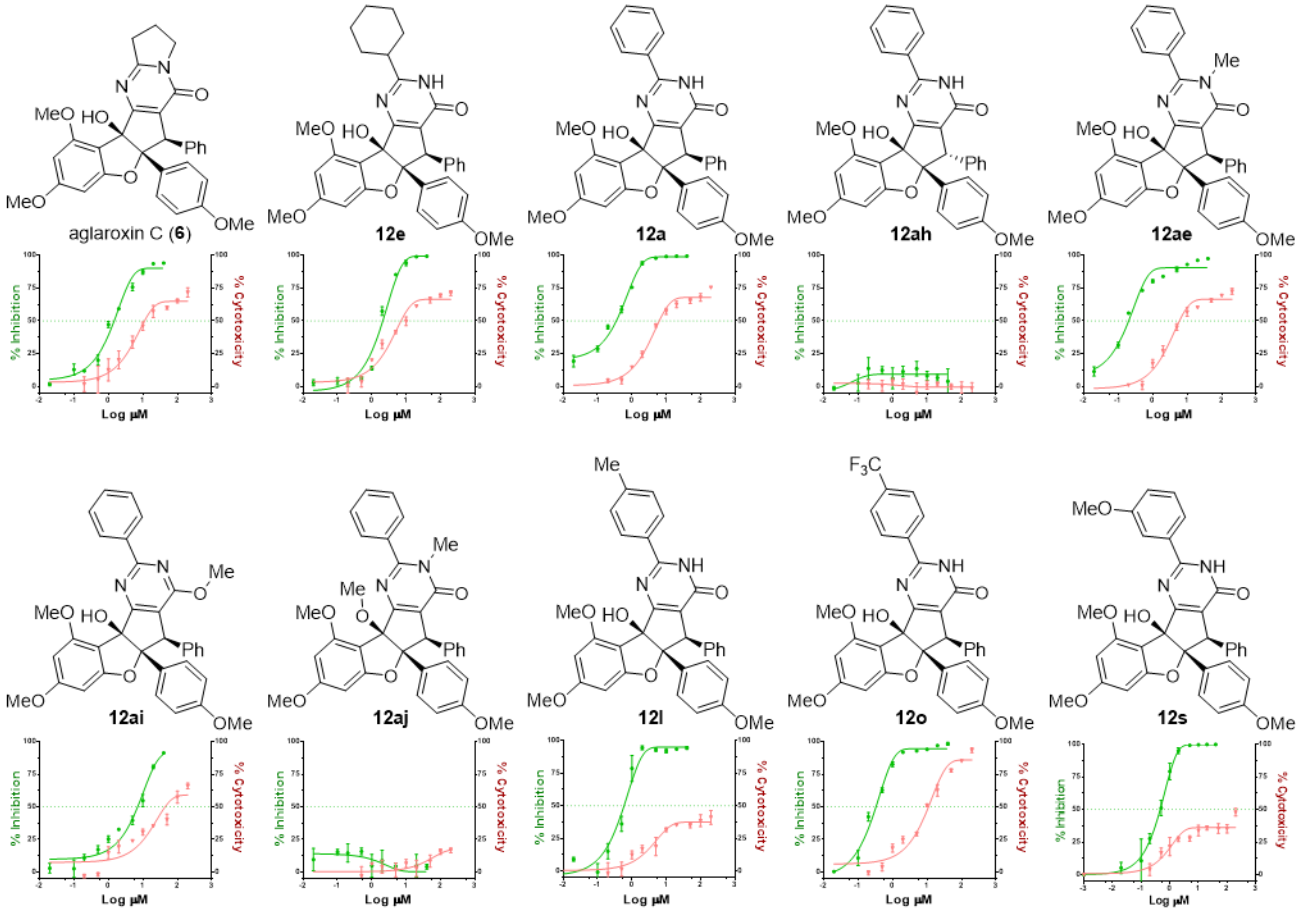

	aglaroxin C (**6**)	**12e**	**12a**	**12ah**	**12ae**	**12ai**	**12aj**	**12l**	**12o**	**12s**
EC_{50}[b] (μM)	1.3	2.5	0.42	n.d.[f]	0.2	9.2	n.d.[f]	0.52	0.24	0.46
CC_{50}[c] (μM)	12	7.5	8.1	n.d.[f]	7.3	37	n.d.[f]	n.d.[g]	10	n.d.[g]
$AUC_{0.2\text{-}200}$[d] cytotoxicity	110	124	125	N/A	123	83	N/A	71	130	90
$AUC_{0.2\text{-}20}$[e] EC/CC	2.3	1.8	2.3	N/A	2.9	2.1	N/A	4.7	3.2	3.3

[a]Absolute EC_{50} and CC_{50} were determined from fitted sigmoid curves; [b] Absolute EC_{50} indicates the concentration of compound that inhibits HCV infection by 50%. For its determination, HCVcc-Luc was added to Huh7.5.1 cells at 37 °C together with serially diluted compounds for 3 h prior to removal. Infected cells were incubated at 37 °C for an additional 48 h prior to luciferase assay (mean of n = 3; error bars, s.d.); [c] Absolute CC_{50} indicates the concentration of compound required to effect 50% cell death. The numbers of viable cells in culture were determined using the CellTiter-Glo Cell Viability Luminescent Assay kit according to the manufacturer's (Promega) instruction (mean of n = 3; error bars, s.d.); [d]$AUC_{0.2\text{-}200}$ (cytotoxicity) is the integration of area under the cytotoxicity curve from 0.2 to 200 μM concentration; [e]$AUC_{0.2\text{-}20}$ (EC/CC) is the ratio (fold-difference) of the integraded area under curve (AUC) values from 0.2 to 20 μM concentration for the effective curve vs. the cytotoxicity curve; [f]n.d. = not determined; no detectable inhibition or cytotoxicity was observed; [g]n.d. = CC_{50} was not determined; some cytotoxicity was observed, but cytotoxicity curve did not reach 50% inhibition.

proved EC_{50}s in the viral infection assay but displayed low cytotoxicity; neither compound reached 50% cell death up to 200 μM concentration (maximum cytotoxicity plateau: 40% and 35% cell death for **12l** and **12s**, respectively). Of note, we observed a similar plateauing of cytotoxicity using aglaroxin C (**6**) and its analogues (**12e**, **12a**, and **12ae**). In contrast, the 4'-trifluoromethylphenyl analog **12o** achieved close to 100% cell death. For a more reliable comparison of cytotoxicities among these compounds, we also calculated the area under the cytotoxicity curve (AUC) by integration,[34] an alternative method for accurately quantifying low cytotoxicity.[35] In this manner, $AUC_{0.2\text{-}200}$ analysis indicates that **12e**, **12a**, and **12ai** share similar cytotoxicities to **6**, whereas **12l** and **12s** exhibit relatively lower cytotoxicities. Extending this analysis to compare the SI among the analogues, we next calculated the $AUC_{0.2\text{-}20}$(EC/CC) ratios, determining that **12ae**, **12l**, **12o**, and **12s** had wider therapeutic windows (0.6 to greater than 2-fold increase in the SI) than **6**. Based on the performance of **12l** and **12s** using these metrics,

we utilized these two lead compounds for further biological investigations including mechanism studies.

To further characterize the mode of action of the two lead compounds **12l** and **12s**, we independently synthesized each of their respective enantiomers and investigated their biological activities in both the HCV viral infection and cytotoxicity assays (Table 5). As expected, only (+)-**12l** and (+)-**12s** displayed HCV inhibition, whereas the other enantiomers (-)-**12l**, and (-)-**12s** were found to be inactive and non-toxic.[26] Interestingly, we noticed that maximum cytotoxicity plateau of both active enantiomer (+)-**12l** and (+)-**12s** increased substantially compared to their racemic counterparts (±)-**12l** and (±)-**12s**. To verify this result, a secondary MTS cell viability assay was also performed on racemic compounds (±)-**12k**, (±)-**12l**, and (±)-**12o**, and showed nearly identical toxicity curves as were observed in the CellTiter-Glo assay.[26] While these results warrant further investigation, they suggest a potential rationale for the observed SI enhancement in which the "inactive" enantiomers may reduce or otherwise mitigate the cytotoxic effects of the active species through an as-yet undefined mechanism.

Table 5. Chirality-Based Biological Profiles of Lead Compounds[a]

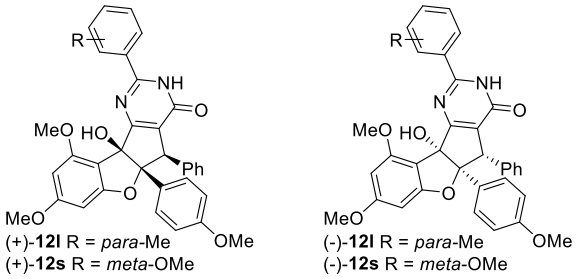

compound	(±)-12l	(+)-12l	(-)-12l	(±)-12s	(+)-12s	(-)-12s
EC_{50}[b] (μM)	0.5	0.3	n.d.[e]	0.5	0.5	n.d.[e]
CC_{50}[c] (μM)	n.d.[d]	10	n.d.[e]	n.d.[d]	7.0	n.d.[e]

[a]EC_{50} and CC_{50} were collected using the same assay in **Table 4** and were calculated based on the fitted sigmoid curves; [b]EC_{50} indicates the concentration of a compound that inhibits 50% HCV infection; [c]CC_{50} indicates the concentration of a compound leads 50% cell death; [d]n.d. = CC_{50} was not determined; some cytotoxicity was observed, but cytotoxicity curve did not reach 50% inhibition; [e]n.d. = not determined; no detectable inhibition or cytotoxicity was observed.

Aglaroxin Analogues Do Not Affect HCV RNA Replication and Translation. We subsequently evaluated the ability of the aglaroxin C analogues to inhibit HCV RNA replication and mRNA translation using an HCV replicon system which harbors a full-length HCV Genotype 1b RNA genome.[36] In replicon cells, HCV RNA replicates and is translated into viral proteins without forming infectious viruses. Hence, this system permits accurate assessment of any effects on viral RNA replication and translation. As shown in Figure 2, compounds (+)-**12l** and (+)-**12s** when used at 2 μM for 3 h did not inhibit HCV RNA replication or protein synthesis. This data implies that the observed inhibitory effects of (+)-**12l** and (+)-**12s** were unlikely due to inhibition of viral RNA replication or mRNA translation. To corroborate these findings, we assembled an *in vitro* translation inhibition assay where a bicistronic reporter mRNA was programmed for translation in Krebs-2 extracts (Figure 3).[37] In this system, translation of the Firefly luciferase (FLuc) translation is cap-dependent whereas Renilla luciferase (RLuc) translation is dependent upon the HCV internal ribosome entry site (IRES) (Fig. 3A). It was observed that translation inhibition of firefly luciferase by **6** and analogues **12l** and **12s** were minimal in comparison with CR-1-31-B (Figure 1, **4**), a highly potent rocaglate translation inhibitor showing strong inhibition of cap-dependent protein synthesis (Figure 3B).[10c] This data suggests that HCV mRNA translation is not inhibited by **6** and its analogues **12l** and **12s**.

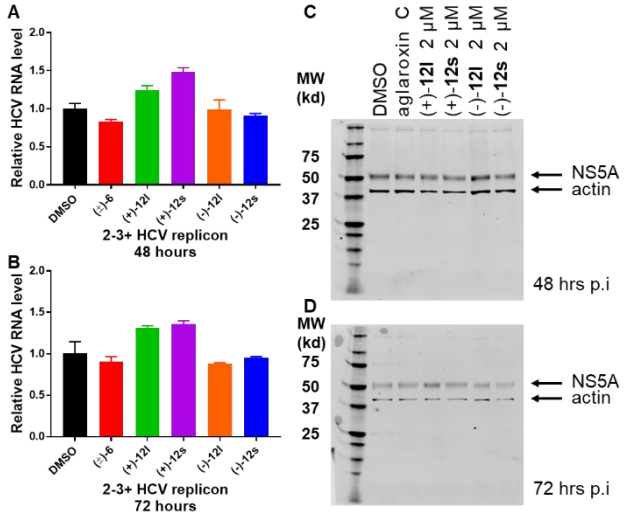

Figure 2. Aglaroxin C (**6**) and analogues (**12l** and **12s**) neither inhibit HCV RNA replication nor protein translation. HCV replicon cell line 2-3+ was treated with indicated compounds for 3 h. Cells were incubated for an additional 48 (**A** & **C**) or 72 h (**B** & **D**). Cellular RNA or protein was isolated for quantifications of HCV viral RNA by real-time PCR (**A** & **B**) or non-structural protein NS5 by western blotting (**C** & **D**).

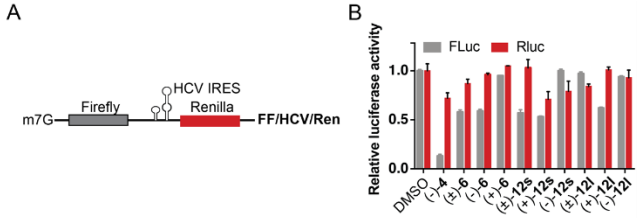

Figure 3. Aglaroxin-type analogues displayed minimal translation inhibition in the comparison to (-)-**4** (CR-1-31-B). (**A**) Schematic representation of the bicistronic reporter FF/HCV/Ren mRNA used to monitor translation. In this system, Firefly luciferase (FLuc) translation is cap-dependent whereas Renilla luciferase (RLuc) expression is HCV-IRES dependent. (**B**) Assessment of cap or HCV dependent translation of FF/HCV/Ren mRNA in the presence of 1 μM of the indicated compounds in Krebs-2 extracts. Results are presented relative to values obtained in the presence of DMSO and expressed as mean ± error of 2 biological replicates.

Aglaroxin Analogues Inhibit HCV Entry. As aglaroxin C was previously reported to inhibit HCV entry,[12] we carried out two sets of experiments to test whether compounds **12l** and **12s** also inhibit viral entry. Firstly, we generated infectious lentiviral pseudotypes bearing glycoproteins of HCV (HCVpp), Chikungunya virus (CHIKVpp), Ebola virus (Ebolapp), and vesicular stomatitis virus (VSVpp). Compositionally, these pseudotyped viruses differ only in viral envelopes because they are packaged using the same lentiviral reporter construct with a separate construct expressing specified viral envelope protein. Hence, the only difference among these pseudoviral particles is the mode of entry, which is dictated by the particular viral glycoprotein found on the viral envelopes. Compounds **12l** and **12s**,

as both the racemates and single (+)-enantiomers, specifically inhibited HCVpp and CHIKVpp but not Ebolapp and VSVpp (Figure 4, A and B). Interestingly, like rocaglamide, compounds (+)-**12l** and (+)-**12s** as well as their racemic versions also inhibited Dengue virus infection (Figure 4C). It is worth mentioning that HCV, Dengue virus, and CHIKV all utilize PHBs to enter cells; further studies are warranted to determine whether compounds **12l** and **12s** directly target PHBs. Secondly, to confirm inhibition of HCV entry, we performed time-of-addition experiments using the lead compounds **12l** and **12s** wherein compounds were added at different times relative to when the virus was added to cells. Similar to **6**, **12l** and **12s** displayed maximal anti-HCV activity when added together with the virus, but partially lost their activity when added 3 h after infection was initiated (Figure 4D). This finding confirmed that **12l** and **12s** are preferentially inhibiting viral entry.

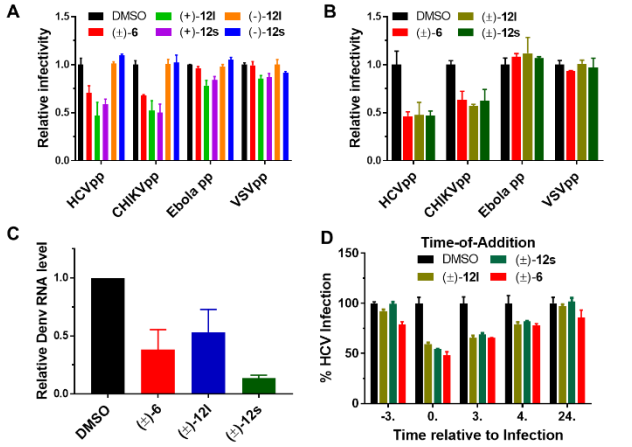

Figure 4. Aglaroxin C (**6**) and its analogues (**12l** & **12s**) inhibit viral entry. (**A**) Huh7.5.1 cells were infected by indicated pseudovirus in the presence of compounds (1 μM) for 3 h. After an additional 48 h infection, cells were lysed for luciferase assay. Relative infectivity was calculated by normalizing against the values obtained from cells treated with DMSO (arbitrarily set to 1.0) (mean ± SD, *$p < 0.05$). (**B**) Same as in a except (±)-**12l** and (±)-**12s** were added at 2 μM. (**C**) Huh7.5.1 cells were infected by Dengue virus (serotype 2, Thailand 16681 strain, MOI 0.1) treated with 2 μM compounds for 3 h. 48 h post-infection, RNA was isolated for quantitative RT-PCR analysis. Viral RNA levels were normalized against GAPDH levels. Data presented are representatives of two independent experiments. (**D**) (±)-**6**, (±)-**12l**, and (±)-**12s** inhibited HCV infection when added together with the virus. Details on this time-of-addition experiment can be found in Supporting Information.

CONCLUSION

In summary, we have developed a second-generation synthesis of aglaroxin C using late-stage, direct pyrimidinone formation of a keto-rocaglate scaffold. Using this method, we have used commercially available amidines as reaction partners to synthesize a library of over forty aglaroxin C analogues. Among newly synthesized analogues, we successfully demonstrated SAR for inhibition of HCV infection and identified two aryl pyrimidinone lead compounds, **12l** and **12s**, which have low cytotoxicities to Huh 7.5.1 cells. Additional biological studies with **12l** and **12s** indicate that the mechanism of inhibition of HCV infection is through inhibition of HCV viral entry, rather than by blocking viral replication and translation. Finally, **12l** and **12s** are also effective against infection of other viruses including Dengue and Chikungunya, both of which have been found to use prohibitins (PHBs) as an entry factor. These studies illustrate the power of chemical synthesis to bias inhibition of HCV viral entry *vs*. translation inhibition and improve properties including therapeutic index. Further studies toward target identification of **12l**, **12s**, and related compounds is currently in progress and will be reported in due course.

ASSOCIATED CONTENT

Supporting Information

Experimental procedures and characterization data for all new compounds described herein, including a CIF file for compound **15**. This material is available free of charge via the Internet at http://pubs.acs.org.

AUTHOR INFORMATION

Corresponding Author

* porco@bu.edu
* tony.wang@fda.hhs.gov

Author Contributions

‡These authors contributed equally.

ACKNOWLEDGMENT

We thank the National Institutes of Health (R01 DK088787 and R35 GM-118173) and the Canadian Institutes of Health Research (FDN-148366) for research support, Dr. Jeffrey Bacon (Boston University) for X-ray crystal structure analyses, Dr. Norman Lee (Boston University) for high-resolution mass spectrometry data, and Nicholas Grigoriadis (Boston University) for preliminary studies NMR (CHE-0619339) and MS (CHE0443618) facilities at Boston University are supported by the NSF. Research at the BU-CMD was supported by NIH grant GM-067041. We thank Dr. Kyle Reichl (Boston University) for proofreading the manuscript.

REFERENCES

(1) Lu King, M.; Chiang, C.-C.; Ling, H.-C.; Fujita, E.; Ochiai, M.; McPhail, A. T. *X*-Ray Crystal Structure of Rocaglamide, a Novel Antileulemic 1*H*-Cyclopenta[*b*]benzofuran from *Aglaia elliptifolia J. Chem. Soc., Chem. Commun.* **1982**, 1150.

(2) For isolation of aglaroxin C, see: (a) Kokpol, U.; Venaskulchai, B.; Simpson, J.; Weavers, R. T. Isolation and *X*-Ray Structure Determination of a Novel Pyrimidinone from *Aglaia odorata*. *J. Chem. Soc., Chem. Commun.* **1994**, 773; (b) Ohse, T.; Ohba, S.; Yamamoto, T.; Koyano, T.; Umezawa, K. Cyclopentabenzofuran Lignan Protein Synthesis Inhibitors from *Aglaia odorata*. *J. Nat. Prod.* **1996**, *59*, 650; (c) Nugroho, B. W.; Edrada, R. A.; Güssregen, B.; Wray, V.; Witte, L.; Proksch, P. Insecticidal Rocaglamide Derivatives from *Aglaia duppereana*. *Phytochemistry* **1997**, *44*, 1455.

(3) For general reviews of rocaglate natural products, see: (a) Ebada, S. S.; Lajkiewicz, N.; Porco, J. A., Jr.; Li-Weber, M.;

Proksch, P. Chemistry and Biology of Rocaglamides (= Flavaglines) and Related Derivatives from *Aglaia Species* (Meliaceae). In *Progress in the Chemistry of Organic Natural Products Vol. 94*; Kinghorn, A. D., Falk, H., Kobayashi, J., Eds.; Springer Vienna: Vienna, **2011**, p 1; (b) Ribeiro, N.; Thuaud, F.; Nebigil, C.; Désaubry, L. Recent Advances in the Biology and Chemistry of the Flavaglines. *Bioorg. Med. Chem.* **2012**, *20*, 1857. (c) Pan, L.; Woodard, J. L.; Lucas, D. M.; Fuchs, J. R.; Kinghorn, A. D. Rocaglamide, Silvestrol and Structurally Related Bioactive Compounds from *Aglaia* Species *Nat. Prod. Rep.* **2014**, *31*, 924.

(4) For reviews of the synthesis of rocaglates, see: (a) Peter, P.; RuAngelie, E.; Rainer, E.; Frank, I. B.; Bambang, W. N. Chemistry and Biological Activity of Rocaglamide Derivatives and Related Compounds in *Aglaia* Species (Meliaceae). *Curr. Org. Chem.* **2001**, *5*, 923; (b) Cai, X.-h.; Xie, B.; Guo, H. Progress in the Total Synthesis of Rocaglamide. *ISRN Org. Chem.* **2011**, *2011*, 7; (c) Zhao, Q.; Abou-Hamdan, H.; Désaubry, L. Recent Advances in the Synthesis of Flavaglines, a Family of Potent Bioactive Natural Compounds Originating from Traditional Chinese Medicine. *Eur. J. Org. Chem.* **2016**, *2016*, 5908.

(5) Hwang, B. Y.; Su, B.-N.; Chai, H.; Mi, Q.; Kardono, L. B. S.; Afriastini, J. J.; Riswan, S.; Santarsiero, B. D.; Mesecar, A. D.; Wild, R.; Fairchild, C. R.; Vite, G. D.; Rose, W. C.; Farnsworth, N. R.; Cordell, G. A.; Pezzuto, J. M.; Swanson, S. M.; Kinghorn, A. D. Silvestrol and Episilvestrol, Potential Anticancer Rocaglate Derivatives from *Aglaia silvestris*. *J. Org. Chem.* **2004**, *69*, 3350.

(6) (a) Cencic, R.; Carrier, M.; Trnkus, A.; Porco, J. A., Jr.; Minden, M.; Pelletier, J. Synergistic Effect of Inhibiting Translation Initiation in Combination with Cytotoxic Agents in Acute Myelogenous Leukemia Cells. *Leukemia Res.* **2010**, *34*, 535; (b) Lin, C.-J.; Nasr, Z.; Premsrirut, Prem K.; Porco, J. A., Jr.; Hippo, Y.; Lowe, Scott W.; Pelletier, J. Targeting Synthetic Lethal Interactions between Myc and the eIF4F Complex Impedes Tumorigenesis. *Cell Rep.* **2012**, *1*, 325; (c) Sadlish, H.; Galicia-Vazquez, G.; Paris, C. G.; Aust, T.; Bhullar, B.; Chang, L.; Helliwell, S. B.; Hoepfner, D.; Knapp, B.; Riedl, R.; Roggo, S.; Schuierer, S.; Studer, C.; Porco, J. A., Jr.; Pelletier, J.; Movva, N. R. Evidence for a Functionally Relevant Rocaglamide Binding Site on the eIF4A–RNA Complex. *ACS Chem. Bio.* **2013**, *8*, 1519; (d) Robert, F.; Roman, W.; Bramoullé, A.; Fellmann, C.; Roulston, A.; Shustik, C.; Porco, J. A., Jr.; Shore, G. C.; Sebag, M.; Pelletier, J. Translation Initiation Factor eIF4F Modifies the Dexamethasone Response in Multiple Myeloma. *PNAS* **2014**, *111*, 13421; (e) Pelletier, J.; Graff, J.; Ruggero, D.; Sonenberg, N. Targeting the eIF4F Translation Initiation Complex: A Critical Nexus for Cancer Development. *Cancer Res.* **2015**, *75*, 250.

(7) (a) Cencic, R.; Carrier, M.; Galicia-Vázquez, G.; Bordeleau, M.-E.; Sukarieh, R.; Bourdeau, A.; Brem, B.; Teodoro, J. G.; Greger, H.; Tremblay, M. L.; Porco, J. A., Jr., Jr.; Pelletier, J. Antitumor Activity and Mechanism of Action of the Cyclopenta[*b*]benzofuran, Silvestrol. *PLOS ONE* **2009**, *4*, e5223; (b) Wolfe, A. L.; Singh, K.; Zhong, Y.; Drewe, P.; Rajasekhar, V. K.; Sanghvi, V. R.; Mavrakis, K. J.; Jiang, M.; Roderick, J. E.; Van der Meulen, J.; Schatz, J. H.; Rodrigo, C. M.; Zhao, C.; Rondou, P.; de Stanchina, E.; Teruya-Feldstein, J.; Kelliher, M. A.; Speleman, F.; Porco, J. A., Jr.; Pelletier, J.; Rätsch, G.; Wendel, H.-G. RNA G-quadruplexes Cause eIF4A-dependent Oncogene Translation in Cancer. *Nature* **2014**, *513*, 65; (c) Chu, J.; Cencic, R.; Wang, W.; Porco, J. A., Jr.; Pelletier, J. Translation Inhibition by Rocaglates Is Independent of eIF4E Phosphorylation Status. *Mol. Cancer Ther.* **2016**, *15*, 136; (d) Langlais, D.; Cencic, R.; Moradin, N.; Kennedy, J. M.; Ayi, K.; Brown, L. E.; Crandall, I.; Tarry, M. J.; Schmeing, M.; Kain, K. C.; Porco, J. A., Jr.; Pelletier, J.; Gros, P. Rocaglates as Dual-targeting Agents for Experimental Cerebral Malaria. *PNAS* **2018**, *115*, e2366.

(8) (a) Iwasaki, S.; Floor, S. N.; Ingolia, N. T. Rocaglates Convert DEAD-box Protein eIF4A into a Sequence-selective Translational Repressor. *Nature* **2016**, *534*, 558; (b) Chu, J.; Galicia-Vázquez, G.; Cencic, R.; Mills, John R.; Katigbak, A.; Porco, J. A., Jr., Jr.; Pelletier, J. CRISPR-Mediated Drug-Target Validation Reveals Selective Pharmacological Inhibition of the RNA Helicase, eIF4A. *Cell Rep.* **2016**, *15*, 2340.

(9) For chemical synthesis of rocaglate natural products, see: (a) Kraus, G. A.; Sy, J. O. A Synthetic Approach to Rocaglamide via Reductive Cyclization of δ-Keto Nitriles. *J. Org. Chem.* **1989**, *54*, 77; (b) Trost, B. M.; Greenspan, P. D.; Yang, B. V.; Saulnier, M. G. An Unusual Oxidative Cyclization. A Synthesis and Absolute Stereochemical Assignment of (-)-Rocaglamide. *J. Am. Chem. Soc.* **1990**, *112*, 9022; (c) Davey, A. E.; Schaeffer, M. J.; Taylor, R. J. K. Enantioselective Synthesis of Cyclopenta[*b*]benzofurans via An Organocatalytic Intramolecular Double Cyclization. *J. Chem. Soc., Chem. Commun.* **1991**, 1137; (d) Davey, A. E.; Schaeffer, M. J.; Taylor, R. J. K. Synthesis of the Novel Anti-leukaemic Tetrahydrocyclopenta[*b*]benzofuran, Rocaglamide and Related Synthetic Studies *J. Chem. Soc., Perkin Trans. 1* **1992**, 2657; (e) Dobler, M. R.; Bruce, I.; Cederbaum, F.; Cooke, N. G.; Diorazio, L. J.; Hall, R. G.; Irving, E. Total Synthesis of (±)-Rocaglamide and Some Aryl Analogues. *Tetrahedron Lett.* **2001**, *42*, 8281; (f) Thede, K.; Diedrichs, N.; Ragot, J. P. Stereoselective Synthesis of (±)-Rocaglaol Analogues. *Org. Lett.* **2004**, *6*, 4595; (g) Gerard, B.; Jones, G.; Porco, J. A., Jr. A Biomimetic Approach to the Rocaglamides Employing Photogeneration of Oxidopyryliums Derived from 3-Hydroxyflavones. *J. Am. Chem. Soc.* **2004**, *126*, 13620; (h) Diedrichs, N.; Ragot, J. P.; Thede, K. A Highly Efficient Synthesis of Rocaglaols by a Novel α-Arylation of Ketones. *Eur. J. Org. Chem.* **2005**, *2005*, 1731; (i) Gerard, B.; Sangji, S.; O'Leary, D. J.; Porco, J. A., Jr. Enantioselective Photocycloaddition Mediated by Chiral Brønsted Acids: Asymmetric Synthesis of the Rocaglamides. *J. Am. Chem. Soc.* **2006**, *128*, 7754; (j) Sous, M. E.; Khoo, M. L.; Holloway, G.; Owen, D.; Scammells, P. J.; Rizzacasa, M. A. Total Synthesis of (−)-Episilvestrol and (−)-Silvestrol. *Angew. Chem. Int. Ed.* **2007**, *46*, 7835; (k) Gerard, B.; Cencic, R.; Pelletier, J.; Porco, J. A., Jr. Enantioselective Synthesis of the Complex Rocaglate (−)-Silvestrol. *Angew. Chem. Int. Ed.* **2007**, *46*, 7831; (l) Malona, J. A.; Cariou, K.; Frontier, A. J. *J. Am. Chem. Soc.* **2009**, *131*, 7560; (m) Magnus, P.; Freund, W. A.; Moorhead, E. J.; Rainey, T. Nazarov Cyclization Initiated by Peracid Oxidation: The Total Synthesis of (±)-Rocaglamide. *J. Am. Chem. Soc.* **2012**, *134*, 6140; (n) Magnus, P.; Freund, W. A.; Moorhead, E. J.; Rainey, T. Formal Synthesis of (±)-Methyl Rocaglate Using an Unprecedented Acetyl Bromide Mediated Nazarov Reaction. *J. Am. Chem. Soc.* **2012**, *134*, 6140; (o) Lajkiewicz, N. J.; Roche, S. P.; Gerard, B.; Porco, J. A., Jr. Enantioselective Photocycloaddition of 3-Hydroxyflavones: Total Syntheses and Absolute Configuration Assignments of (+)-Ponapensin and (+)-Elliptifoline. *J. Am. Chem. Soc.* **2012**, *134*, 13108; (p) Stone, S. D.; Lajkie-

wicz, N. J.; Whitesell, L.; Hilmy, A.; Porco, J. A., Jr. Biomimetic Kinetic Resolution: Highly Enantio- and Diastereoselective Transfer Hydrogenation of Aglain Ketones to Access Flavagline Natural Products. *J. Am. Chem. Soc.* **2015**, *137*, 525; (q) Wang, W.; Clay, A.; Krishnan, R.; Lajkiewicz, N. J.; Brown, L. E.; Sivaguru, J.; Porco, J. A., Jr. Total Syntheses of the Isomeric Aglain Natural Products Foveoglin A and Perviridisin B: Selective Excited-State Intramolecular Proton-Transfer Photocycloaddition. *Angew. Chem. Int. Ed.* **2017**, *56*, 14479.

(10) For representative studies of rocaglate analogues from academia, see: (a) Roche, S. P.; Cencic, R.; Pelletier, J.; Porco, J. A., Jr. Biomimetic Photocycloaddition of 3-Hydroxyflavones: Synthesis and Evaluation of Rocaglate Derivatives as Inhibitors of Eukaryotic Translation. *Angew. Chem. Int. Ed.* **2010**, *49*, 6533; (b) Thuaud, F.; Ribeiro, N.; Gaiddon, C.; Cresteil, T.; Désaubry, L. Novel Flavaglines Displaying Improved Cytotoxicity. *J. Med. Chem.* **2011**, *54*, 411; (c) Rodrigo, C. M.; Cencic, R.; Roche, S. P.; Pelletier, J.; Porco, J. A., Jr., Synthesis of Rocaglamide Hydroxamates and Related Compounds as Eukaryotic Translation Inhibitors: Synthetic and Biological Studies. *J. Med. Chem.* **2012**, *55*, 558; (d) Hawkins, B. C.; Lindqvist, L. M.; Nhu, D.; Sharp, P. P.; Segal, D.; Powell, A. K.; Campbell, M.; Ryan, E.; Chambers, J. M.; White, J. M.; Rizzacasa, M. A.; Lessene, G.; Huang, D. C. S.; Burns, C. J. Simplified Silvestrol Analogues with Potent Cytotoxic Activity. *ChemMedChem* **2014**, *9*, 1556; (e) Lajkiewicz, N. J.; Cognetta, A. B.; Niphakis, M. J.; Cravatt, B. F.; Porco, J. A., Jr. Remodeling Natural Products: Chemistry and Serine Hydrolase Activity of a Rocaglate-Derived β-Lactone. *J. Am. Chem. Soc.* **2014**, *136*, 2659; (f) Wang, W.; Cencic, R.; Whitesell, L.; Pelletier, J.; Porco, J. A., Jr. Synthesis of Aza-Rocaglates via ESIPT-Mediated (3+2) Photocycloaddition. *Chem. Eur. J.* **2016**, *22*, 12006; (g) Zhao, Q.; Tijeras-Raballand, A.; de Gramont, A.; Raymond, E.; Désaubry, L. Bioisosteric Modification of Flavaglines. *Tetrahedron Lett.* **2016**, *57*, 2943.

(11) For representative medicinal remodeling of rocaglates from industry, see: (a) Bruce, I.; Cooke, N. G.; Diorazio, L. J.; Hall, R. G.; Irving, E. Synthesis of the Carbocyclic Analogue of (±)-Rocaglamide. *Tetrahedron Lett.* **1999**, *40*, 4279; (b) Liu, T.; Nair, S. J.; Lescarbeau, A.; Belani, J.; Peluso, S.; Conley, J.; Tillotson, B.; O'Hearn, P.; Smith, S.; Slocum, K.; West, K.; Helble, J.; Douglas, M.; Bahadoor, A.; Ali, J.; McGovern, K.; Fritz, C.; Palombella, V. J.; Wylie, A.; Castro, A. C.; Tremblay, M. R. Synthetic Silvestrol Analogues as Potent and Selective Protein Synthesis Inhibitors. *J. Med. Chem.* **2012**, *55*, 8859.

(12) (a) Liu, S.; Wang, W.; Brown, L. E.; Qiu, C.; Lajkiewicz, N.; Zhao, T.; Zhou, J.; Porco, J. A., Jr.; Wang, T. T. A Novel Class of Small Molecule Compounds that Inhibit Hepatitis C Virus Infection by Targeting the Prohibitin-CRaf Pathway. *EBioMedicine* **2015**, *2*, 1600; (b) Wang, T. T.; Liu, S.; Wang, W.; Lajkiewicz, N.; Porco, J. A., Jr Aglaroxin C and Derivatives as HCV Entry Inhibitors. US patent **2018** US 10,085,988 B1.

(13) For other natural product inhibitors of HCV viral entry, see: (a) Calland, N.; Sahuc, M.-E.; Belouzard, S.; Pène, V.; Bonnafous, P.; Mesalam, A. A.; Deloison, G.; Descamps, V.; Sahpaz, S.; Wychowski, C.; Lambert, O.; Brodin, P.; Duverlie, G.; Meuleman, P.; Rosenberg, A. R.; Dubuisson, J.; Rouillé, Y.; Séron, K. Polyphenols Inhibit Hepatitis C Virus Entry by a New Mechanism of Action. *J. Virol.* **2015**, *89*, 1005; (b) Lin, L.-T.; Chung, C.-Y.; Hsu, W.-C.; Chang, S.-P.; Hung, T.-C.; Shields, J.; Russell, R. S.; Lin, C.-C.; Li, C.-F.; Yen, M.-H.; Tyrrell, D. L. J.; Lin, C.-C.; Richardson, C. D. Saikosaponin b2 is a Naturally Occurring Terpenoid That Efficiently Inhibits Hepatitis C Virus Entry. *J. Hepatol.* **2015**, *62*, 541; (c) Qian, X.-J.; Zhang, X.-L.; Zhao, P.; Jin, Y.-S.; Chen, H.-S.; Xu, Q.-Q.; Ren, H.; Zhu, S.-Y.; Tang, H.-L.; Zhu, Y.-Z.; Qi, Z.-T. A Schisandra-Derived Compound Schizandronic Acid Inhibits Entry of Pan-HCV Genotypes into Human Hepatocytes. *Sci. Rep.* **2016**, *6*, 27268; (d) Bose, M.; Kamra, M.; Mullick, R.; Bhattacharya, S.; Das, S.; Karande, A. A. A Plant-derived Dehydrorotenoid: a New Inhibitor of Hepatitis C Virus Entry. *FEBS Lett.* **2017**, *591*, 1305.

(14) Kuadkitkan, A.; Wikan, N.; Fongsaran, C.; Smith, D. R. Identification and Characterization of Prohibitin as a Receptor Protein Mediating DENV-2 Entry into Insect Cells. *Virology* **2010**, *406*, 149.

(15) Wintachai, P.; Wikan, N.; Kuadkitkan, A.; Jaimipuk, T.; Ubol, S.; Pulmanausahakul, R.; Auewarakul, P.; Kasinrerk, W.; Weng, W.; Panyasrivanit, M.; Paemanee, A.; Kittisenachai, S.; Roytrakul, S.; Smith, D. R. Identification of Prohibitin as a Chikungunya Virus Receptor Protein. *J. Med. Virol.* **2012**, *84*, 1757.

(16) Vos, T.; Allen, C.; Arora, M.; Barber, R. M.; Bhutta, Z. A.; Brown, A.; Carter, A.; Casey, D. C.; Charlson, F. J.; Chen, A. Z.; Coggeshall, M.; Cornaby, L.; Dandona, L.; Dicker, D. J.; Dilegge, T.; Erskine, H. E.; Ferrari, A. J.; Fitzmaurice, C.; Fleming, T.; Forouzanfar, M. H.; Fullman, N.; Gething, P. W.; Goldberg, E. M.; Graetz, N.; Haagsma, J. A.; Hay, S. I.; Johnson, C. O.; Kassebaum, N. J.; Kawashima, T.; Kemmer, L.; Khalil, I. A.; Kinfu, Y.; Kyu, H. H.; Leung, J.; Liang, X.; Lim, S. S.; Lopez, A. D.; Lozano, R.; Marczak, L.; Mensah, G. A.; Mokdad, A. H.; Naghavi, M.; Nguyen, G.; Nsoesie, E.; Olsen, H.; Pigott, D. M.; Pinho, C.; Rankin, Z.; Reinig, N.; Salomon, J. A.; Sandar, L.; Smith, A.; Stanaway, J.; Steiner, C.; Teeple, S.; Thomas, B. A.; Troeger, C.; Wagner, J. A.; Wang, H.; Wanga, V.; Whiteford, H. A.; Zoeckler, L.; Abajobir, A. A.; Abate, K. H.; Abbafati, C.; Abbas, K. M.; Abd-Allah, F.; Abraham, B.; Abubakar, I.; Abu-Raddad, L. J.; Abu-Rmeileh, N. M. E.; Ackerman, I. N.; Adebiyi, A. O.; Ademi, Z.; Adou, A. K.; Afanvi, K. A.; Agardh, E. E.; Agarwal, A.; Kiadaliri, A. A.; Ahmadieh, H.; Ajala, O. N.; Akinyemi, R. O.; Akseer, N.; Al-Aly, Z.; Alam, K.; Alam, N. K. M.; Aldhahri, S. F.; Alegretti, M. A.; Alemu, Z. A.; Alexander, L. T.; Alhabib, S.; Ali, R.; Alkerwi, A. a.; Alla, F.; Allebeck, P.; Al-Raddadi, R.; Alsharif, U.; Altirkawi, K. A.; Alvis-Guzman, N.; Amare, A. T. Global, Regional, and National Incidence, Prevalence, and Years Lived with Disability for 310 Diseases and Injuries, 1990–2015: a Systematic Analysis for the Global Burden of Disease Study 2015. *The Lancet* **2016**, *388*, 1545.

(17) Denniston, M. M.; Jiles, R. B.; Drobeniuc, J.; Klevens, R. M.; Ward, J. W.; McQuillan, G. M.; Holmberg, S. D. Chronic Hepatitis C Virus Infection in the United States, National Health and Nutrition Examination Survey 2003 to 2010. *Ann. Intern. Med.* **2014**, *160*, 293.

(18) Wang, H.; Naghavi, M.; Allen, C.; Barber, R. M.; Bhutta, Z. A.; Carter, A.; Casey, D. C.; Charlson, F. J.; Chen, A. Z.; Coates, M. M.; Coggeshall, M.; Dandona, L.; Dicker, D. J.; Erskine, H. E.; Ferrari, A. J.; Fitzmaurice, C.; Foreman, K.; Forouzanfar, M. H.; Fraser, M. S.; Fullman, N.; Gething, P. W.; Goldberg, E. M.; Graetz, N.; Haagsma, J. A.; Hay, S. I.; Huynh, C.; Johnson, C. O.; Kassebaum, N. J.; Kinfu, Y.; Kulikoff, X. R.; Kutz, M.; Kyu, H. H.; Larson, H. J.; Leung, J.; Liang, X.; Lim, S. S.; Lind, M.; Lozano, R.; Marquez, N.; Mensah, G. A.;

Mikesell, J.; Mokdad, A. H.; Mooney, M. D.; Nguyen, G.; Nsoesie, E.; Pigott, D. M.; Pinho, C.; Roth, G. A.; Salomon, J. A.; Sandar, L.; Silpakit, N.; Sligar, A.; Sorensen, R. J. D.; Stanaway, J.; Steiner, C.; Teeple, S.; Thomas, B. A.; Troeger, C.; VanderZanden, A.; Vollset, S. E.; Wanga, V.; Whiteford, H. A.; Wolock, T.; Zoeckler, L.; Abate, K. H.; Abbafati, C.; Abbas, K. M.; Abd-Allah, F.; Abera, S. F.; Abreu, D. M. X.; Abu-Raddad, L. J.; Abyu, G. Y.; Achoki, T.; Adelekan, A. L.; Ademi, Z.; Adou, A. K.; Adsuar, J. C.; Afanvi, K. A.; Afshin, A.; Agardh, E. E.; Agarwal, A.; Agrawal, A.; Kiadaliri, A. A.; Ajala, O. N.; Akanda, A. S.; Akinyemi, R. O.; Akinyemiju, T. F.; Akseer, N.; Lami, F. H. A.; Alabed, S.; Al-Aly, Z.; Alam, K.; Alam, N. K. M.; Alasfoor, D.; Aldhahri, S. F.; Aldridge, R. W.; Alegretti, M. A.; Aleman, A. V.; Alemu, Z. A.; Alexander, L. T. Global, Regional, and National Life Expectancy, All-cause Mortality, and Cause-specific Mortality for 249 Causes of Death, 1980-2015: a Systematic Analysis for the Global Burden of Disease Study 2015. *The Lancet* **2016**, *388*, 1459.

(19) For a comprehensive review of DAAs for HCV, see: Götte, M.; Feld, J. J. Direct-acting Antiviral Agents for Hepatitis C: Structural and Mechanistic Insights. *Nat. Rev. Gastroenterol. Hepatol.* **2016**, *13*, 338.

(20) Xiao, F.; Fofana, I.; Thumann, C.; Mailly, L.; Alles, R.; Robinet, E.; Meyer, N.; Schaeffer, M.; Habersetzer, F.; Doffoël, M.; Leyssen, P.; Neyts, J.; Zeisel, M. B.; Baumert, T. F. Synergy of Entry Inhibitors with Direct-acting Antivirals Uncovers Novel Combinations for Prevention and Treatment of Hepatitis C. *Gut* **2015**, *64*, 483.

(21) Romano, K. P.; Ali, A.; Aydin, C.; Soumana, D.; Özen, A.; Deveau, L. M.; Silver, C.; Cao, H.; Newton, A.; Petropoulos, C. J.; Huang, W.; Schiffer, C. A. The Molecular Basis of Drug Resistance against Hepatitis C Virus NS3/4A Protease Inhibitors. *PLOS Pathog.* **2012**, *8*, e1002832.

(22) (a) Tong, X.; Le Pogam, S.; Li, L.; Haines, K.; Piso, K.; Baronas, V.; Yan, J.-M.; So, S.-S.; Klumpp, K.; Nájera, I. In Vivo Emergence of a Novel Mutant L159F/L320F in the NS5B Polymerase Confers Low-Level Resistance to the HCV Polymerase Inhibitors Mericitabine and Sofosbuvir. *J. Infect. Dis.* **2014**, *209*, 668; (b) Walker, A.; Filke, S.; Lübke, N.; Obermeier, M.; Kaiser, R.; Häussinger, D.; Timm, J.; Bock, H. H. Detection of a Genetic Footprint of the Sofosbuvir Resistance-associated Substitution S282T after HCV Treatment Failure. *Virol. J.* **2017**, *14*, 106.

(23) For a recent review of current HCV entry inhibitor development, see: Qian, X.-J.; Zhu, Y.-Z.; Zhao, P.; Qi, Z.-T. Entry Inhibitors: New Advances in HCV Treatment. *Emerg. Microbes Infect.* **2016**, *5*, e3.

(24) He, S.; Li, K.; Lin, B.; Hu, Z.; Xiao, J.; Hu, X.; Wang, A. Q.; Xu, X.; Ferrer, M.; Southall, N.; Zheng, W.; Aubé, J.; Schoenen, F. J.; Marugan, J. J.; Liang, T. J.; Frankowski, K. J. Development of an Aryloxazole Class of Hepatitis C Virus Inhibitors Targeting the Entry Stage of the Viral Replication Cycle. *J. Med. Chem.* **2017**, *60*, 6364.

(25) Yueh, H.; Gao, Q.; Porco, J. A.; Beeler, A. B. A Photochemical Flow Reactor for Large Scale Syntheses of Aglain and Rocaglate Natural Product Analogues. *Bioorg. Med. Chem.* **2017**, *25*, 6197.

(26) See the Supporting Information for complete details.

(27) For approved drugs containing the pyrimidinone substructure and their synthesis, see: a) risperidone: Kim, D.-m.; Kang, M.-S.; Kim, J. S.; Jeong, J.-H. An Efficient Synthesis of Risperidonevia Stille Reaction: Antipsychotic, 5-HT_2, and Dopamine-D_2-antagonist. *Arch. Pharm. Res.* **2005**, *28*, 1019; b) paliperidone: Solanki, P. V.; Uppelli, S. B.; Pandit, B. S.; Mathad, V. T. An Improved and Efficient Process for the Production of Highly Pure Paliperidone, a Psychotropic Agent, via DBU Catalyzed N-Alkylation. *ACS Sustainable Chem. Eng.* **2013**, *1*, 243; c) Fimasartan: Kim, T. W.; Yoo, B. W.; Lee, J. K.; Kim, J. H.; Lee, K.-T.; Chi, Y. H.; Lee, J. Y. Synthesis and Antihypertensive Activity of Pyrimidin-4(3*H*)-one Derivatives as Losartan Analogue for New Angiotensin II Receptor Type 1 (AT_1) Antagonists. *Bioorg. Med. Chem. Lett.* **2012**, *22*, 1649.

(28) For selected synthesis of natural products containing pyrimidinones, see: (a) Doveston, R. G.; Steendam, R.; Jones, S.; Taylor, R. J. K. Total Synthesis of an Oxepine Natural Product, (±)-Janoxepin. *Org. Lett.* **2012**, *14*, 1122; (b) Santos, M. F. C.; Harper, P. M.; Williams, D. E.; Mesquita, J. T.; Pinto, É. G.; da Costa-Silva, T. A.; Hajdu, E.; Ferreira, A. G.; Santos, R. A.; Murphy, P. J.; Andersen, R. J.; Tempone, A. G.; Berlinck, R. G. S. Anti-parasitic Guanidine and Pyrimidine Alkaloids from the Marine Sponge *Monanchora arbuscular*. *J. Nat. Prod.* **2015**, *78*, 1101.

(29) For the Traube purine synthesis, see: (a) Traube, W. Ueber Guanidinderivate Zweibasischer Säuren. *Ber. Dtsch. Chem. Ges.* **1893**, *26*, 2551; (b) Traube, W.; Schottländer, F.; Goslich, C.; Peter, R.; Meyer, F. A.; Schlüter, H.; Steinbach, W.; Bredow, K. Über Ortho-diamino-pyrimidine und ihre Überführung in Purine. *Ann. Chem.* **1923**, *432*, 266.

(30) For selected pyrimidinone syntheses from 1,3-dicarbonyl substrates, see: (a) Lal, B.; D'Sa, A. S.; Kulkarni, B. K.; de Souza, N. J. A Convenient One-pot Entry into Novel 2-Substituted-6,7-dihydro-4H-Pyrimido(2,1-a) Isoquinolin-4-ones. *Tetrahedron* **1990**, *46*, 1323; (b) Venkatesan, A. M.; Levin, J. I.; Baker, J. S.; Chan, P. S.; Bailey, T.; Coupet, J. Substituted 4H-Pyrido[1,2-a]pyrimidin-4-one Angiotensin II Receptor Antagonists. *Bioorg. Med. Chem. Lett.* **1994**, *4*, 183; (c) Taylor, E. C.; Zhou, P.; Tice, C. M. 6-Trifluoromethanesulfonyloxy-4(3H)-pyrimidinones as Versatile Intermediates for the Synthesis of 6-Functionalized 4(3H)-Pyrimidinones. *Tetrahedron Lett.* **1997**, *38*, 4343; (d) Puig-de-la-Bellacasa, R.; Giménez, L.; Pettersson, S.; Pascual, R.; Gonzalo, E.; Esté, J. A.; Clotet, B.; Borrell, J. I.; Teixidó, J. Diverse Combinatorial Design, Synthesis and *In Vitro* Evaluation of New HEPT Analogues as Potential Non-nucleoside HIV-1 Reverse Transcription Inhibitors. *Eur. J. Med. Chem.* **2012**, *54*, 159; (e) Guirado, A.; Alarcón, E.; Vicente, Y.; Andreu, R.; Bautista, D.; Gálvez, J. A New Convenient Synthetic Approach to Diarylpyrimidines. *Tetrahedron* **2016**, *72*, 3922

(31) (a) Katritzky, A. R.; Yousaf, T. I. A C-13 Nuclear Magnetic Resonance Study of the Pyrimidine Synthesis by the Reactions of 1,3-Dicarbonyl Compounds with Amidines and Ureas *Can. J. Chem.* **1986**, *64*, 2087. (b) Katritzky, A. R.; Ostercamp, D. L.; Yousaf, T. I. The Mechanisms of Heterocyclic Ring Closures. *Tetrahedron* **1987**, *43*, 5171.

(32) For imidoyl ketene generation and subsequent cyclization, see: (a) Ham, S.; Birney, D. M. Imidoylketene: An *ab Initio* Study of Its Conformations and Reactions. *J. Org. Chem.* **1996**, *61*, 3962; (b) Alajarín, M.; Ortín, M.-M.; Sánchez-Andrada, P.; Vidal, Á.; Bautista, D. From Ketenimines to Ketenes to Quinolones: Two Consecutive Pseudopericyclic Events. *Org. Lett.* **2005**, *7*, 5281; (c) Abe, T.; Kida, K.; Yamada, K. A Copper-

Catalyzed Ritter-type Cascade via Iminoketene for the Synthesis of Quinazolin-4(3*H*)-ones and Diazocines. *Chem. Commun.* **2017**, *53*, 4362.
(33) Schönherr, H.; Cernak, T. Profound Methyl Effects in Drug Discovery and a Call for New C-H Methylation Reactions. *Angew. Chem. Int. Ed.* **2013**, *52*, 12256.
(34) Dye, J. F.; Somers, S. S.; Guillou, P. J. Simplified Quantitation of Cytotoxicity by Integration of Specific Lysis against Effector Cell Concentration at a Constant Target Cell Concentration and Measuring the Area Under the Curve. *J. Immunol. Methods* **1991**, *138*, 1.
(35) (a) Sheeran, T. P.; Jackson, F. R.; Dawes, P. T.; Collins, M.; Shadforth, M. F. Measurement of Natural Killer Cell Cytotoxicity by Area Under a Cytotoxic Curve: A Method Suitable for Rheumatoid Arthritis. *J. Immunol. Methods* **1988**, *115*, 95; (b) Brown, C.; Havener, T.; Everitt, L.; McLeod, H.; Motsinger-Reif, A. A Comparison of Association Methods for Cytotoxicity Mapping in Pharmacogenomics. *Front. Genet.* **2011**, *2*; (c) Huang, S.; Pang, L. Comparing Statistical Methods for Quantifying Drug Sensitivity Based on In Vitro Dose-Response Assays. *Assay Drug Dev. Technol.* **2012**, *10*, 88.
(36) Scholle, F.; Li, K.; Bodola, F.; Ikeda, M.; Luxon, B. A.; Lemon, S. M. Virus-Host Cell Interactions during Hepatitis C Virus RNA Replication: Impact of Polyprotein Expression on the Cellular Transcriptome and Cell Cycle Association with Viral RNA Synthesis. *J. Virol.* **2004**, *78*, 1513.
(37) Novac, O.; Guenier, A. S.; Pelletier, J. Inhibitors of Protein Synthesis Identified by a High Throughput Multiplexed Translation Screen. *Nucleic Acids Res.* **2004**, *32*, 902.

Table of Contents